Feasible options for point-to-point passenger transport with rocket propelled reusable launch vehicles

Steffen Callsen*, Jascha Wilken, Sven Stappert, Martin Sippel

Deutsches Zentrum für Luft- und Raumfahrt (DLR), Robert-Hooke-Straße 7, 28359 Bremen, Germany, *Steffen.Callsen@dlr.de*
* Corresponding Author

Abstract

For the first time in spaceflight history the flight of a fully reusable launch system with rocket propulsion appears possible within the next couple of years. Apart from the implications for the orbital launch market, a fully reusable system could also enable an entirely new class of commercial point-to-point transport on Earth. Rocket propelled point-to-point systems promise the ability to transport passengers or cargo to any suitable landing site on Earth with extremely short travel times (typically less than 90 minutes). In this study the primary focus is on DLR-SART's SpaceLiner 7 vehicle concept with an initial comparison to Starship, currently being developed by SpaceX.

The trajectories are identified using multi-objective optimization with evolutionary algorithms. These allow the identification of a solution space with regard to multiple objectives, in this case minimal overflight of populated areas and minimal peak heat flux, while still respecting other constraints (e.g. structural loads). The population disturbance is computed by using a global population density database and integrating the number of people along the flight track. Ideally, the solution space consists of a pareto-front which correlates to the most optimal solutions possible for all objectives.

The mission analysis identifies various feasible trajectories around the world. Primarily, these routes are going along less populated areas such as the oceans and the polar regions. Especially the latter enable large longitudinal changes during the flight and consequently connecting distant places on Earth. The critical routes are large longitudinal crossings around the equator where land masses must be overflown. These shall be reconsidered and/or improved in the future.

Comparing SpaceLiner to Starship, it is found that the mission profiles vary significantly. While SpaceLiner uses its high lift-to-drag ratio in the higher atmosphere to manoeuvre around large land masses, Starship can only follow the direct route. In contrast, Starship flies higher into space and thereby might avoid having large population disturbances on ground. Only the re-entry and landing are critical as it does not have significant cross range capability. As a design option for the next iteration of the SpaceLiner development, SpaceLiner 8, it is planned to assess the possibility of using a smaller wing to follow a similar coast through space like Starship and have a steep re-entry at the end of the flight instead of a prolonged glide.

Keywords: SpaceLiner, Starship, Point-to-Point, hypersonic transportation, trajectories, multi-objective optimization

Acronyms/Abbreviations

DLR	German Aerospace Center
GPWv4	Gridded Population of the World, v4
NASA	National Aeronautics and Space Administration
SART	Space Launcher Systems Analysis
SLME	SpaceLiner Main Engine

1. Introduction

The introduction of cost-effective, fully-reusable rocket launch systems could lead to a novel commercial point-to-point transportation market on Earth. Both cargo and passengers could be transported around Earth in typically less than 90 minutes.

However, finding connections between major global financial and economic centres with rocket-propelled systems is not trivial as many constraints must be met, for example environmental, structural and thermal constraints. Furthermore, it is desirable to reduce the impact of the flights on the general population.

In order to study these trajectories with all their constraints and objectives, a multi-objective optimization using evolutionary algorithms is introduced. These are envisioned to find solutions in a complex environment with multiple constraints and objectives without relying on a good initial guess.

Additionally, the noise disturbance of the flights is analysed by introducing a population density map of the World. Furthermore, the flights are optimized regarding a minimization of said disturbance by rerouting over unpopulated areas.

In this study, the trajectories of two vehicles will be analysed – DLR-SART's SpaceLiner 7 concept and the currently being developed and built SpaceX Starship. The main focus of this paper will be the SpaceLiner. Starship trajectories will also be shown and compared to the SpaceLiner, but with less detail. A more detailed Starship trajectory analysis created with the same method is published in [1].

2. Vehicle description

The two applicable vehicles are described in this section: SpaceLiner 7 and Starship. A short overview of the architecture and relevant subsystems is given. Additionally, the general layout of a typical trajectory is described.

2.1 SpaceLiner 7-3

The SpaceLiner is a concept for a high-speed Earth point-to-point passenger transport system as well as a satellite launcher internally developed at DLR (see Fig. 1) [2, 3]. It could enable low-cost space transportation while at the same time revolutionizing ultra-long-distance travel between different points on Earth. Travel times for the longest distances (e.g. Europe – Australia) are expected to be about 90 minutes. In case of the orbital transportation system, it is designed as a fully-reusable two-stage system with an additional kick-stage in place of the passenger capsule. This system is described in more detail in [4].

Fig. 1. Rendering of the SpaceLiner passenger stage in gliding flight over Alaska

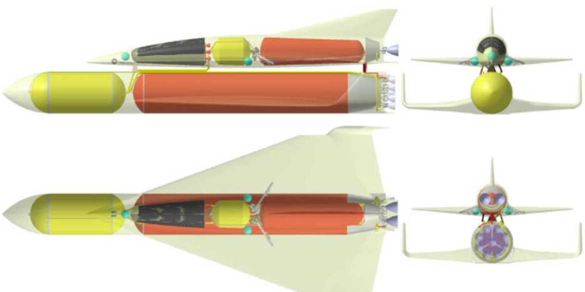

Fig. 2. Sketch of SpaceLiner 7-3 launch configuration with passenger stage.

Architecturally, the passenger version consists of a fully reusable booster and passenger stage arranged in parallel at lift-off as shown in Fig. 2. The main dimensions of the 7-3 booster configuration are listed in Table 1, while the major geometry data of the passenger stage is summarized in Table 2.

Table 1. Geometrical data of SpaceLiner 7-3 booster

	Parameter
Length	82.3 m
Wingspan	36.0 m
Height	8.7 m
Fuselage diameter	8.6 m
Wing leading edge angles	82 / 61 / 43 degree
Wing pitch angle	3.5 degree
Wing dihedral angle	0 degree

Table 2. Geometrical data of SpaceLiner 7-3 passenger stage

	Parameter
Length	65.6 m
Wingspan	33.0 m
Height	12.1 m
Fuselage diameter	6.4 m
Wing leading edge angle	70 degree
Wing pitch angle	0.4 degree
Wing dihedral angle	2.65 degree

Total dry mass of the SpaceLiner 7-3 launch configuration is estimated at 327 tons for the passenger version with a total propellant loading of 1502 tons. The resulting lift-off weight is 1829 tons including passengers.

Both stages are powered by the SpaceLiner Main Engine (SLME) which runs on a full-flow staged combustion cycle with liquid hydrogen as fuel and liquid oxygen as oxidizer. The booster stage has nine engines, while the passenger stage contains two. As all engines are active from lift-off until MECO, the engine is designed to work from sea-level to vacuum conditions. A propellant crossfeed from the booster to the passenger stage is foreseen up to separation to reduce the overall size of the configuration [5]. The current status of the detailed SLME design is shown in [6].

The aerodynamic design of the SpaceLiner passenger stage is the key enabler of the flight routes discussed in this study. Its single-delta wing shape is optimized for high lift-to-drag ratios of up to 3.5 in the hypersonic range allowing for long flights at high altitudes above 70 km. More detailed analysis of the aerodynamic and aerothermodynamic design is published in [7, 8, 9, 10].

The general layout of a SpaceLiner point-to-point trajectory can be separated into the powered ascent and the unpowered descent. It takes off vertically from a launch pad with all engines operating and crossfeed between the booster stage and orbiter enabled. During the ascent, individual engines are switched off once an acceleration threshold of 2.5 g is crossed, which is done for passenger comfort. After burn-out of the booster at about Mach 12, the two stages separate and the passenger stage continues on its own with full tanks due to the propellant crossfeed. The booster then re-enters the atmosphere and is recovered by means of 'In-Air-Capturing', where the stage is caught by an airplane with a rope connection system and afterwards towed back to the launch site. This method is studied in detail in the EC funded project FALCon [11].

After the Passenger stage burn is completed, which is generally below 100 km altitude and Mach numbers above 20, it performs a gliding descent to the target location, primarily using its high hypersonic lift-to-drag ratio to create lift at altitudes between 70 and 90 km. During this flight phase, it can vary its angle of attack and bank angle to perform manoeuvres towards the landing site. Once it arrives at the target location, a horizontal landing on a runway is performed.

The SpaceLiner upper stage also has an alternative version for orbital satellite deliveries. The volume of the passenger capsule is replaced with the payload and an additional kick-stage for deliveries into high energetic orbits such as GTO. The two-stage-to-orbit performance to a low Earth orbit without the kick-stage is approximately 26 tons. Using the kick-stage, it can deliver about 8.3 tons to a GTO while landing the orbiter again at the launch site after a complete circumnavigation of Earth. [4]

2.2 Starship

Starship is a space transportation system currently in development by SpaceX that is targeting to be the first ever fully reusable launcher system (see Fig. 3) [12]. It is a two stage to orbit system with a reusable payload mass to LEO of around 100 tons. It is proposed to be refuelled in orbit and shall eventually carry humans to Mars. Additionally, it is contracted to carry humans from an orbit around the Moon to its surface within the Artemis program [13]. Additionally, SpaceX has proposed to use Starship for Earth point-to-point transport similar to the SpaceLiner [14]. The main dimensions and masses of the Starship system are shown in Table 3, where the first stage is called Super Heavy and the second stage Starship.

Fig. 3. View of Starship system on launch pad [15]

Table 3. Geometric data of SpaceX Starship system [13]

	Super Heavy	Starship
Length	70 m	50 m
Diameter	9 m	9 m
Propellant mass	3400 t	1200 t

It is powered by the Raptor engine, which is the first flown full-flow staged combustion engine. It utilizes liquid methane as fuel and liquid oxygen as oxidizer. In the current version, 33 engines are placed on the first stage and six on the upper stage (3 vacuum optimized, 3 sea-level optimized).

Starship also performs a vertical take-off from a launch pad. However, the two stages are arranged in a tandem-configuration, which does not allow for the parallel burning of both stages. The two-stage ascent injects Starship into a slightly suborbital trajectory with significantly higher altitudes than SpaceLiner. Starship then coasts in space until it re-enters the atmosphere.

The re-entry is performed with a high angle of attack of approximately 70 degrees for maximum drag in the higher atmosphere in order to reduce the peak heat flux. Once the majority of kinetic energy is discarded, Starship flies or rather falls with an angle of attack up to 90 degrees for the so-called Skydive-manoeuvre. Only close to the ground, the engines are re-lit and the vehicle is rotated 90 degrees and performs a vertical landing.

A critical analysis of the Starship system by DLR can be found in [16], from which the system data necessary for the trajectory analysis shown in chapter 4 is taken.

3. Methodology

An innovative approach to mission design is explored for the trajectories computed in this study. This methodology is explained in this chapter, first outlining the multi-objective optimization procedure. Also, the utilized population density database is explained before the boundary conditions are described.

3.1 Multi-objective optimization with evolutionary algorithms

Trajectories for hypersonic rocket-propelled spacecraft are inherently complex to generate as a large number of constraints and objectives shall be met. In the past, SpaceLiner trajectories have largely been created with manual 'by-hand' guidance or local optimization when a good manual initial solution was available. Considering the global optimization problem, both methods have significant disadvantages and are unlikely to provide the best solution, especially when the population living underneath is considered.

For this reason, global optimization methods were investigated, of which multi-objective optimizations based on evolutionary algorithms proved to be the most promising. In literature, the multi-objective optimization methodology seems to have been primarily used for isolated parts of space vehicle trajectories like launch vehicle ascents [17], re-entry [18] and orbital trajectories [19]. In some cases, evolutionary algorithms have been successfully used for a combination of ascent and descent trajectory optimization [20].

In this case, the optimization of a point-to-point trajectory essentially combines a launch vehicle ascent with an orbital re-entry. These rocket propelled reusable launch system concepts for point-to-point transport are quite rare which is why not much research on such trajectories has been performed.

Additionally, one major feature of this study is utilizing the world-wide population density database GPWv4 (see section 3.2) for analysing the population disturbance along the trajectory during the optimization. While such a database has been used for studies on population avoidance for supersonic flights [21], it was implemented as a constraint and not part of the objective function.

After having investigated multiple optimization procedures, it was found that multi-objective optimization provided better results than single objective optimization (e.g. differential evolution [22]).

Multi-objective optimization using evolutionary algorithms enables solving problems with a large solution space by computing a large number of results (in this case trajectories) simultaneously with different, randomly chosen parameter values and evaluating these based on constraints and objectives set beforehand [23]. Subsequently, solutions considered as good are then used in the next evolutionary generation as a starting point. Additionally, evolutionary principles such as crossover of two solutions or mutation of a single solution are applied. The goal of these is both finding better solutions as well as making them more diverse.

The optimization problem at hand can be described as follows:

Minimize peak heat flux(x), population integral(x) subject to:

- Peak dynamic pressure < 40 kPa
- Target latitude difference < 0.4 degree
- Target longitude difference < 0.4 degree

where x is the vector of decision variables consisting of 47 elements

The decision variables are listed below, with their boundaries described in section 3.3.

- Launch azimuth (degree)
- Pitching rate (degree per second)
- Burn time of second stage solo flight (seconds)
- Angle of attack at beginning of second stage solo flight (degree)
- Angle of attack at end of second stage solo flight (degree)
- Horizontal thrust vector control at beginning of second stage solo flight (degree)
- Horizontal thrust vector control at end of second stage solo flight (degree)
- Angle of attack during descent at 20 evenly spaced time points (degree)
- Bank angle during descent at 20 evenly spaced time points (degree)

The controls during the ascent of the first stage are kept constant except for the launch azimuth and pitching rate. During the first stage flight, the angle of attack is kept close to zero at all times to avoid high mechanical loads on the structure. The first stage burns through all the available propellant. Additionally, a fixed throttling scheme is used to keep the acceleration and thereby passenger comfort at acceptable levels.

At first, the optimizer is working towards finding a feasible solution, meaning that all constraints are met. In this case, this implies that the flight path ends at the specified target region and certain flight parameters (e.g. dynamic pressure) are below their defined threshold. Once a feasible solution is found, the solutions are improved according to the defined objectives. For the SpaceLiner case, optimization is done for two objectives: Minimizing the maximum experienced heat flux on the vehicle as well as the integral of the population encountered on the way (described in the next section). While optimizing the heat flux below its design limit might not be necessary for the feasibility of the flight, it is desired as it reduces the loads on the vehicle leading to potential lengthening of its lifespan and reduction of refurbishment cost.

The problem at hand is optimized for both objectives. Thus, there will be at least two solutions: One with a minimum heat flux and one with a minimum population integral. Additionally, a number of solutions laying in-between these extrema might be found creating a diverse result. At best, these solutions comprise of the pareto-front which showcases the most optimal outcomes in a large space of feasible options (see Fig. 4). Optimizing until the actual Pareto front is found is estimated to exceed the current computational resources and time available for each trajectory, especially due to the ‘chaotic’ population density map which does not allow for an obvious improvement pattern. However, the trajectories are always propagated until the solution is estimated to be reasonably close to the Pareto front and feasible for the vehicles.

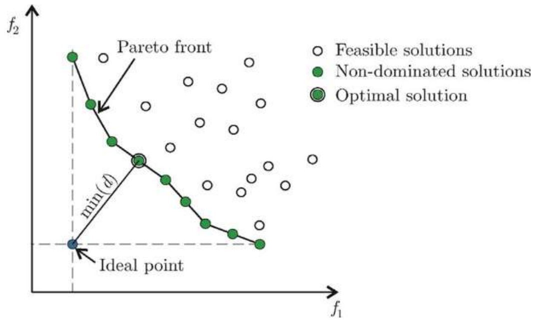

Fig. 4. Explanation of the Pareto front [24]

In most cases, the trajectories on the limits of the objectives are not the most desirable choice for implementation as there tends to be a big compromise on the other objective (e.g. lowest heat flux, but flying over more densely populated areas and vice versa). Here, the user must make a trade-off and find the overall best solution for this application case, which is usually performed based on background information not available to the optimizer.

For this study, the trajectories are propagated with a population size of 2000 along initially 1000 generations. If the results were found to be unsatisfactory after the initial 1000 generations, the optimization was allowed to run for an additional 1000 generations before assessing the quality of the solutions again.

Because of the highly irregular distribution of the Earth's population (see section 3.2) and the sensitivity of the trajectory problem, it is not deemed feasible to identify global optima within available computation times. Instead, the goal is to identify good candidate solutions that represent feasible trajectories. Thus, the quality of the solutions was not assessed with an automated convergence criterion, but instead manually checked with regard to heat flux (which has a physical lower limit) and the flight path with regard to the population distribution.

The magnitude of the population and propagated generations are currently limited by the performance and computation time required for the optimization. The current optimization requires substantial computational effort. Propagating an optimization along 1000 generations with the available workstation (2x Intel Xeon Platinum 8260L with 24 cores each, using 44/48 cores) takes about 16 hours.

There is room for improvement regarding the optimization time as the interface between the optimization Python framework and the separate simulation program is not optimal due to file-based data transfer. Enabling the Python framework to directly call the Fortran routines of the simulation program would likely yield a significant speed increase.

3.2 Population density database

The two vehicles analysed in this study utilize high amounts of energy for lift-off and the subsequent ascent flight. Later, they re-enter the atmosphere and dissipate this energy to slow down. Both flight phases lead to high amount of noise and potentially the experience of sonic booms along their flight path. Consequently, the trajectories shall at best avoid conglomerations of people in the form of large cities. For this reason, a population density database called GPWv4 is introduced, which shall be used to optimize for lowest population impact along the trajectory.

GPWv4 (Gridded Population of the World, Version 4) is a population database of the whole world managed and maintained by NASA's Socioeconomic Data and Applications Center and the Center for International Earth Science Information Network at Columbia University [25]. The data is organized in a gridded form along longitudes and latitudes in a maximum resolution of 30 arc-seconds (approximately 1 km at the equator). As this application does not require such a high precision, a lower resolution of 15 arc-minutes is chosen (approximately 28 km at the equator), which also aids with computing effort. An exemplary view of the population density map in this resolution can be seen in Fig. 5.

Along the whole flight trajectory, the population density below the flight track is computed in steps of at maximum 5 km in order to gain sufficient accuracy in the grid. Because population avoidance is primarily done due to noise pollution, this is only checked below 80 km altitude during the descent. Furthermore, below Mach 1 the population density is also not examined due to the absence of a sonic boom. The 80 km threshold is chosen based on sonic boom research. Both sonic boom overpressure prediction methodologies [26] as well as measurements from the Space Shuttle [27] indicate overpressure reaching the ground up to an altitude of about 76 km. The threshold of 80 km is chosen as a worst-case scenario with a margin towards the 76 km altitude.

During the ascent, the population density is computed below 80 km altitude due to the noise of the running engines. Above 80 km, it is assumed that the engine noise does not reach the ground in a significant amplitude. In order to investigate the overall impact on the population of one flight, the integral of the population density along the flight track and to the side is calculated. Thus, a lower value indicates that less people are subjected to flight noise.

Besides the subject of noise pollution, the factor of safety for the general population has to be considered. For the purposes of this study, it is assumed that the SpaceLiner system satisfies the safety requirements to be allowed to fly over certain populated land areas. As a passenger transport system, it inherently has to satisfy high safety requirements. However, it shall avoid highly populated areas as best as possible, which is supported by the chosen methodology. Thus, the population avoidance is primarily focused on noise pollution, with the added bonus of a safety increase.

In the database there can be high population density value differences between single grid points (e.g. one contains a city, the adjacent one only farm land or water). Hence, the optimizer could choose flight routes very close to a city while computing low population numbers. As a consequence, the GPWv4 population density map is manipulated so that each grid point displays the worst-case value in a 50 km radius (see Fig. 6). With this new map, the optimizer is inclined to search for routes which are considered sufficiently far away from population centres.

The route solutions are in the end again analysed based on the original population density map to explore the actual impact on the population within a 100 km wide corridor (50 km to the left, 50 km to the right of the flight path). Based on the overflown area, a total number of potentially disturbed people can be calculated. 50 km in each direction is estimated to be reasonable without the actual knowledge of the sound dissipation. The actual launch noise and sonic boom analysis shall be part of future work.

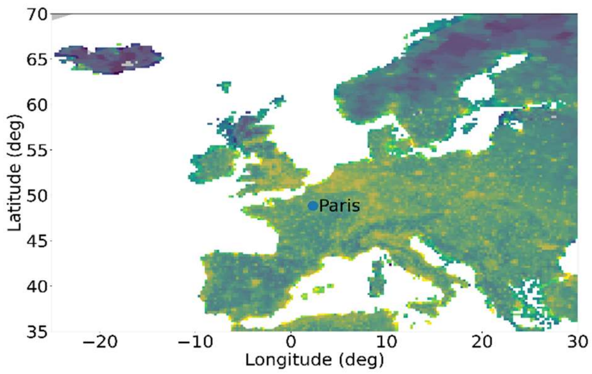

Fig. 5. GPWv4 Population density map of Europe, normalized between 1 (purple) and 1000 people/km² (yellow)

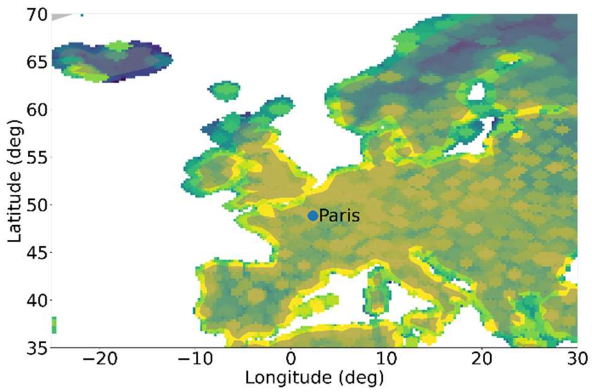

Fig. 6. GPWv4 Population density map of Europe with worst-case value in a radius of 50 km, normalized between 1 (purple) and 1000 people/km² (yellow)

The overall quality of this data is considered to be good as it provides values for the whole Earth that can be easily used and implemented. However, it shall be mentioned that in some countries – especially ones with large land area – the data is not as detailed. In these cases, large areas have the same population density data value in the database. Thus, it can be assumed that the number of people living there is scaled to a large area. As this is primarily done in areas with few people, it is not considered to be problematic for this study.

3.3 Boundary conditions

The following Table 4 shows the lower and upper boundaries of the controls defined for the optimization of the SpaceLiner flight profiles. In Table 5, the flight constraints are listed. Within the following results the heat flux is estimated for the stagnation point with a modified Chapman equation as shown in the following equation (1). Here, ρ is the local density at the respective altitude according to the US standard atmosphere 1976, ρ_R is a reference density value of 1.225 kg/m³, $R_{N,r}$ is reference nose radius (here 1 m), R_N is the vehicle nose radius (assumed to be 0.2m), v is the vehicle's velocity and v_r is a reference velocity of 10000 m/s.

$$\dot{q} = 20254.4 \frac{W}{cm^2} \cdot \sqrt{\frac{\rho}{\rho_R} \frac{R_{N,r}}{R_N}} \left(\frac{v}{v_r}\right)^{3.05} \quad (1)$$

At this point in time, the listed constraint value of 2 MW/m² is an assumption based on previous design work. However, defining a solid boundary is not simple as it depends on a number of aspects (e.g. design of the thermal protection system, temporal distribution of the heat loads). Most flight routes stay significantly below that value between about 1.0 and 1.5 MW/m². Higher heat fluxes have repercussions on the overall system design which were not analysed within this work and would require another iteration step.

The equivalent control boundaries and constraints for Starship are listed in Table 6 and 7. Additionally, Table 8 displays the assumed allowed launch azimuths for the chosen launch sites. The sites are selected based on already existing launch infrastructure as well as geographically interesting locations for such a transportation system launch. The launch azimuths are defined based on the available corridor above water surrounding the location. No powered ascent above any large cities is permitted. If already established launch sites are considered (e.g. Cape Canaveral SFB, USA), then the officially designated headings are chosen.

Table 4. SpaceLiner control lower and upper boundaries

	Boundaries
Pitching rate	0.2°/s – 0.6°/s
Burn time S2 solo flight	150 s – 203 s
Angle of Attack S2 burn	-20° – 20°
Horizontal TVC S2 burn	-8° – 8°
Angle of Attack descent	0° – 20°
Bank angle descent	-50° – 50°

Table 5. SpaceLiner flight constraints

	Constraints
Max. dynamic pressure	40 kPa
Peak heat flux	2 MW/m²
Target location (lat, lon)	± 0.4°

Table 6. Starship control lower and upper boundaries

	Boundaries
Pitching rate	0.1°/s – 0.4°/s
Burn time S2 solo flight	94 s – 281 s
Angle of Attack S2 burn	-30° – 30°
Angle of Attack descent	40° – 70°

Table 7. Starship flight constraints

	Constraints
Max. dynamic pressure	60 kPa
Max. lateral load	3.5 g_0
Target location	± 1°

Table 8. Launch sites and allowed heading range

	Heading range
Nordholz, Germany	260° – 350°
Rockhampton, Australia	-35° – 140°
Cape Canaveral SFB, USA [28]	35° – 120°
Vandenberg SFB, USA [28, 29]	140° - 301°
Wallops FF, USA [28]	90° – 160°
Noto Peninsula, Japan	-115° – 30°
Shengsi Islands/Shanghai, China	-20° – 180°
Tirunelvi District, India	140° – 225°
Overberg District, South Africa	110° – 290°
Campos dos Goytacazes, Brazil	30° – 210°
CSG, Kourou, French Guiana [30]	-5° – 95°

4. Point-to-Point Trajectories

Trajectories of both vehicles are analysed in this section regarding their overall feasibility. Furthermore, the advantages and disadvantages of the multi-objective optimization is discussed based on the examples at hand. At the end, this topic is expanded with a comparison of an exemplary route between Starship and SpaceLiner.

4.1 SpaceLiner

In this subsection, a few selected SpaceLiner trajectory solutions found by the multi-objective optimization tool are shown and discussed in detail. Subsequently, all currently computed SpaceLiner trajectories are shown and explored in a world map.

The first example shown in Fig. 7 is Japan to Germany. The launch site in Japan is on Noto peninsula within the Ishikawa Prefecture. The landing site is Nordholz airport near Cuxhaven, Germany. Five different trajectories are found with two distinct flight routes which will be explained below.

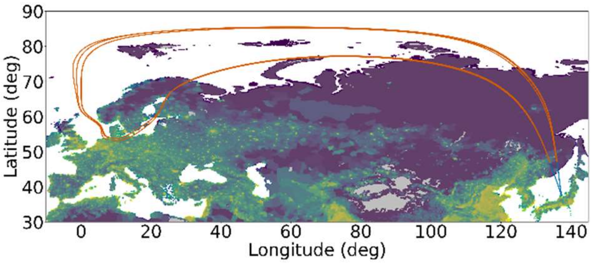

Fig. 7. Trajectory options Japan – Germany

In general, all launch ascents are executed with a northward heading flying over the Arctic avoiding larger population centres in the north-eastern part of China. Flying into the Arctic puts all flight paths north of the great circle connecting Japan and Germany which would be the shortest route available. By doing so, large accumulations of population are avoided.

Due to optimizing for both minimum heat flux and minimum population, two distinct flight routes are found. The more northern flight route avoids basically all population on route by flying over rural Russia, the Arctic and finally through the northern Atlantic and the North Sea.

In contrast, the other flight route does not go as far North and instead of flying around Norway, it enters Europe via Finland and the Baltic Sea over sparsely populated land areas. The flight to Nordholz then follows the Baltic Sea around Sweden and Denmark into Germany either south of Hamburg over Mecklenburg-Vorpommern or north over Schleswig-Holstein.

In order to analyse the trade-off of this route selection, the pairs of the peak heat flux and population integral are shown in Table 9.

Table 9. Optimization results for route Japan – Germany

Case	Peak heat flux (MW/m²)	Population integral (million)
1	1.30	0.288
2	1.27	0.611
3	1.26	0.973
4	1.15	6.341
5	1.09	9.973

The encountered population for the three northern routes is between 0.29 and 0.97 million, while achieving peak heat fluxes between 1.26 and 1.30 MW/m². For the route along the Baltic sea, the optimizer achieves heat fluxes as low as 1.09 MW/m², which is why these are considered in the optimization trade-off. However, the large negative effect of such a route is the overflown population which for these cases lies between 6.34 and 9.97 million, over 10 times higher than the alternative route.

In this case, trading off between the two different flight routes, the choice would go to the longer flight route around Norway as the disturbed population is significantly lower and the heat flux is still within the SpaceLiner design boundaries. Additionally, getting regulatory approval to fly over any densely populated land area is deemed challenging at this point in time. However, it is beneficial that the algorithm correctly identifies both options.

The second SpaceLiner example showcased here is Australia to the northern part of the US East Coast (Wallops flight facility in Virginia). The relevant descent part of the flight is shown in Fig. 8.

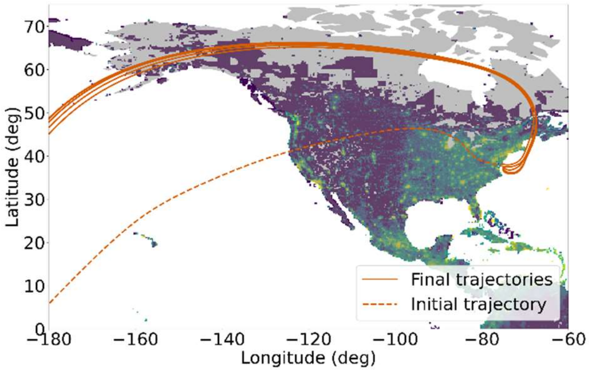

Fig. 8. Trajectory options Australia – Virginia, USA

This case is a good example for a trajectory, where a good solution regarding low population disturbance is further away from the great circle connection and the optimizer needs to be creative to find this solution. This can be difficult as it usually finds the first solution somewhere around the great circle and improves from there. Mutating to a widely differing launch azimuth with a subsequent complicated descent flight and still hitting the target area is doable but unlikely. This is why the launch azimuth is a critical parameter for finding good solutions.

The dashed line in Fig. 8 shows the trajectory found by the optimizer after 1000 generations when the parameter bounds are set as defined in Table 8. It flies directly over the continental US and arrives to the target area from the west. Given its flight route, it is able to find a corridor with reasonable population disturbance of around 10 million people by avoiding the major population centres like Chicago and Washington D.C. It also chooses to fly over highly forested areas like the Appalachian Mountains. Nevertheless, it is still optimizing a local optimum.

Instead, for the final trajectory result, the boundaries for the launch azimuth are narrowed to constrain the trajectories to a more northern path. Here, the optimizer finds great solutions regarding the population disturbance. The launch leads to a long flight over the Pacific, then passes over Alaska and northern Canada. After traversing the Hudson Bay and Québec, the SpaceLiner enters the Atlantic at the US-Canadian border and flies around the populated East Coast to Wallops. Only between 0.47 and 1.75 million people are disturbed on this route which is one magnitude lower than the initial trajectory. The achieved heat flux for the lowest population disturbance of 0.47 million is 1.38 MW/m², while it is 1.07 MW/m² for the highest disturbance of 1.75 million people. The value-pairs are shown in Table 10.

Table 10. Optimization results for route Australia – Virginia, USA

Case	Peak heat flux (MW/m²)	Population integral (million)
1	1.11	0.759
2	1.13	0.747
3	1.08	0.733
4	1.07	1.751
5	1.38	0.474
6	1.28	0.725

Beyond these exemplary routes, many other connections have been analysed which are displayed on a world map in Fig. 9. These all connect major economic, financial and population centres of the world. When avoiding flyover of largely populated areas as best as possible, the layout of Earth has certain limitations regarding SpaceLiner flight routes which will be discussed in the following.

In general, the best areas for flight routes are oceans or other bodies of water like the North Sea. Additionally, the polar regions in the North and South are equally sparsely populated and offer the opportunity for large longitudinal crossings, for example from the Pacific Ocean to the Northern Atlantic.

In contrast, when flying over land the flight routes should avoid populated areas as much as possible. This is especially problematic in the northern hemisphere which contains about two thirds of the land area but almost 90 percent of the population [31]. Furthermore, the land mass and the people living there extend into higher latitudes beyond 60 degrees while in the southern hemisphere most landmasses do not extend beyond 50 degrees latitude. As a consequence, it is far easier to connect separate continents in the southern hemisphere by flying over the southern Oceans and Antarctic region. Additionally, because the Indian Ocean extends from

Antarctica to India itself, even people living on landmasses in the northern hemisphere can be served with these southern-oriented flight routes. The same is true for South America, where places in the northern hemisphere are served from Kourou via the North pole.

Fig. 10 shows the high influence of the northern polar region with regards to connecting the northern hemisphere. A large majority of the flight routes traverses this region.

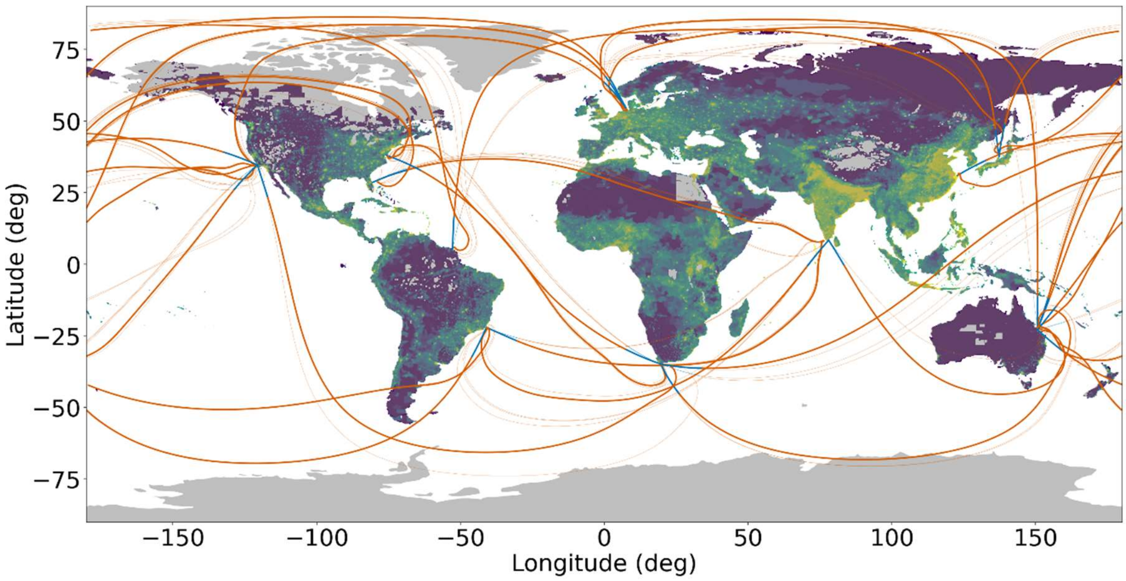

Fig. 9. World map with all computed SpaceLiner trajectories (Blue: Ascent, Orange: Descent) including population density, normalized between 1 (purple) and 1000 people/km² (yellow)

Fig. 10. All trajectories from above the North Pole

Overall, the computed routes can be sorted in roughly four groups that are identifiable in the world map:

- Flights solely in northern or southern hemisphere via polar region and adjacent Oceans
- Flights crossing from one hemisphere to the other and using the polar regions for large longitudinal crossings (mainly Arctic)
- Flights in the equator region with large longitudinal crossings
- Flights above an Ocean (crossing hemispheres or not)

Because of the launch azimuth boundaries of the chosen launch sites, it is not always possible to have a round trip connection. A round trip connection example is Australia – Germany and vice versa where the flight route can be served in both directions. In contrast, India – Australia is a one-way route as the flight goes around the continent and Australia's launch heading range towards the north and east does not allow a launch back to India. Instead, in such a case the SpaceLiner vehicle could be part of a route system connecting multiple stops around the Earth. Here, this could for example be India – Australia – Florida – India.

Beyond the heading range boundaries, the quality of a launch site in terms of surrounding land mass as well as location on the world map is a critical factor.

The chosen location in Australia is adjacent to the vast Pacific Ocean and allows launching to a large variety of places, e.g. towards the North to the Arctic and thereby the northern Atlantic, towards the East to all other American-Pacific launch sites as well as to the South-East to reach the southern Atlantic. It only has weaknesses towards the West.

In contrast, the currently chosen launch site in Japan basically only allows for launches towards the North to the Arctic. While this enables flights towards Europe and the northern part of South America, launching in the direction of anywhere in the Pacific is not possible but could be desirable.

The selection of suitable launch sites is not final and substantial potential for optimization within future work exists.

All investigated flight routes and their minimum and maximum population disturbance values are listed in Table 9. The large majority of the flights fly over less than 5 million people. The average of the minimum and maximum values are 1.43 million and 4.08 million respectively, placing most routes in the lower seven digits area. However, analysing the median, it shows that 50 percent of the minimum disturbance values are below 0.37 million and 1.49 million for the maximum value. Thus, the distribution is not symmetrical and the average is distorted by routes like Florida – India with exceptionally high numbers. As a consequence, these routes shall be reconsidered or improved in the future.

On the lower end of the results, routes like Brazil – Australia offer values below 100.000 people. Almost the whole flight is performed over Oceans and few people live in the coastal areas overflown by the vehicle (Falkland Islands and the southern tip of South America). Only the South Island of New Zealand is crossed directly. However, the optimizer manages to find a route through mostly mountainous and wooded areas.

Table 11. List of all SpaceLiner flight routes

		Pop. Disturbance	
Nr.	Route	Min.	Max.
1	Germany – Australia	0.01 M	0.02 M
2	Australia – Germany	1.18 M	4.03 M
3	Australia – Florida, US	0.44 M	1.28 M
4	Florida, US – India	9.97 M	24.6 M
5	India – Australia	1.70 M	9.28 M
6	Australia – Virginia, US	0.47 M	1.75 M
7	Germany – Japan	3.00 M	3.50 M
8	Japan – Germany	0.29 M	9.97 M
9	Germany – California, US	0.13 M	0.25 M
10	China – California, US	3.62 M	5.74 M
11	California, US – China	0.55 M	0.57 M
12	Brazil – India	0.07 M	3.41 M
13	India – Brazil*	1.59 M	1.83 M
14	Brazil – Australia	0.09 M	0.47 M
15	Australia – Brazil	1.06 M	1.15 M
16	Kourou – Japan	0.19 M	1.69 M
17	Japan – Kourou	0.17 M	0.31 M
18	Virg., US – South Africa	0.01 M	0.05 M
19	South Africa - Australia	0.03 M	0.04 M
20	South Africa – Virg., US	3.99 M	6.66 M
21	Cal., US – South Africa	0.17 M	0.20 M
22	South Africa – Cal., US	5.45 M	20.5 M
23	Australia – California, US	0.01 M	0.25 M
24	California, US – Australia	0.01 M	0.46 M
$\bar{x}$	Mean (Average)	1.43 M	4.08 M
$\tilde{x}$	Median	0.37 M	1.49 M

*Because the population density data of the Maldives is found to be incorrect (significantly too high, on the order of two magnitudes), the disturbance numbers are calculated without it and a standard worst-case value of 0.54 million is added which corresponds to the total population of the Maldives

The route Florida – India is also a good example for the system impact of these analyses. In fact, the optimizer found population disturbances lower than the 9.97 million displayed in Table 11 which were as low as 2.23 million.

For these routes, the optimizer finds trajectories with lower disturbances by introducing skipping manoeuvres. Instead of a continuous flightpath in the higher airspace below 100 km, the vehicle ascends higher into space (e.g. 120-150 km) before it enters the atmosphere. When hitting the atmosphere, sufficient lift is created to ascend into space again, although with a lower higher apogee. Thus, the vehicle is 'skipping' the atmosphere along the trajectory. Because the noise disturbance is absent at these higher altitudes, it is able to fly over densely populated areas without impacting them. The drawback of this strategy are the severely higher heat fluxes experienced by the vehicle during the several re-entries, which exceed the currently estimated thermal design boundaries for the SpaceLiner and are consequently discarded from the selection.

Adapting the SpaceLiner design to accommodate higher peak heat flux and performing one large exoatmospheric coast in space with a single re-entry manoeuvre is planned for the SpaceLiner 8 design phase.

While routes with high disturbance values shall be further improved if possible, the general impact on the population should be discussed in future work regarding the limits that can be acceptable for the population living in these areas. Overall, finding flight routes that traverse up to approximately 18,500 km of Earth and do not fly over more than a few million people within a 100 km wide corridor is considered a good result.

However, the definition of the 100 km corridor is based on an estimation. The actual amplitude and propagation of the sonic boom depends on the flight parameters of the vehicles, such as Mach number, altitude, angle of attack and flight path angle. Not all overflight disturbances are equally strong. Ideally, this would be evaluated within the optimization loop but that is computationally expensive. But a detailed analysis of a flight's distribution and overpressure magnitude of the sonic boom on the ground as a posterior analysis could give further insight into the challenges surrounding this topic and the acceptable level of population overflight.

4.2 Starship

The models used for the evaluation of the Starship mission are based on DLR reverse engineering from publicly available information. The general vehicle model as well as the performance evaluation for orbital missions is published in [16] while the point-to-point missions are discussed in more detail in [1] as well as a comparison of the vehicle properties and re-entry behaviour. The following paragraphs briefly summarize the assumptions used for the Starship mission optimization.

In general, the Starship has some cross-range capability through aerodynamic means, but significantly less than the SpaceLiner Orbiter. Theoretically, the flight azimuth can also be changed through additional burns, but this will necessitate substantial additional Δv capability of the system. Thus, the Starship missions are assumed to not include banking manoeuvres in order to reduce the degree of freedoms for the optimizer. This significantly reduces the computational resources needed for a mission evaluation.

The trajectory integration is terminated once the vehicle reaches Mach 1. The landing burn itself is not simulated, since from a performance perspective it will be virtually identical in each case, due to the previous skydiving phase. Thus, a fixed propellant budget is assumed. For this optimization 100-ton payload were assumed. For a passenger stage the payload will have to include the life support system as well as the structure in which the passengers will be seated.

For this payload the mission was optimized for minimal peak heat flux. Since the Starship is not able to laterally avoid population centers, only missions with unpopulated areas for the initial ascent as well as the final portion of the descent were evaluated.

4.3 Comparison of SpaceLiner and Starship routes

The following paragraphs compare the trajectories of the SpaceLiner and Starship based on a specific mission. [1] contains parametric studies for identical re-entry conditions as well as for a mission from California to Shanghai.

While the powered ascent of the SpaceLiner and Starship is relatively similar, the rest of the flight to the target location is not. Thus, a comparison of both vehicles is performed. An interesting use case for this is found in the route Brazil to India. Additionally, the reverse route India to Brazil is looked at briefly.

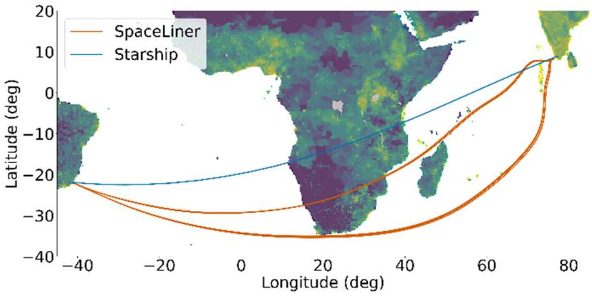

Fig. 11. Trajectory options comparison between SpaceLiner and Starship for Brazil – India

The map-view in Fig. 11 shows the general route of the trajectory options. Because of Starship's aerodynamic design, its flight trajectory is very limited in its cross-range capability. Consequently, it follows the great circle connecting the launch and landing site. It is not able to divert around any significant landmasses on the route. However, as most of the flight is performed at higher altitudes, it can be expected that less people are actually disturbed. Only during the re-entry, a sonic boom will reach the ground along its flight path.

In contrast, the SpaceLiner uses its lift-capability to divert from the great circle and fly routes over less populated areas. In the current optimization solution, one route crosses Africa along the border of South Africa with Namibia and Botswana until it flies over Mozambique. However, the more advantageous route in terms of population disturbance follows a more southern path around the Horn of Africa and Madagascar. In this case, the optimizer considers both options as the first one has a lower peak heat flux.

For the final part of the trajectory, the Maldives are the primary area to avoid. While Starship is required to cross them, all SpaceLiner routes avoid the island group either to the North or to the East.

When comparing the re-entry profiles of both vehicles, the differences are immediately identifiable but not as large as expected (see Fig. 12). While the SpaceLiner stays below 80 km using its high lift-to-drag ratio at hypersonic speeds, Starship ascends to about 100 km on its suborbital flightpath.

Afterwards, during re-entry the SpaceLiner trajectory follows a relatively continuous path. Here, a disadvantage of the current optimization routine is identified which does not optimize for the smoothest flightpath possible. This is especially recognizable in the later parts of the trajectory where the heat flux is already below the peak region and the optimizer has no incentive to further improve the smoothness of the flightpath.

In comparison, Starship also creates significant amounts of lift at around 60-70 km in order to decelerate in the higher atmosphere and limit the heat flux. However, because of its significantly higher drag, it cannot glide as far. Once decelerated, Starship loses altitude quickly.

Starship only stays above 80 km in the first half of the flight. At the beginning of the second half, it is still over Africa and thus noise disturbance for the population is to be expected. The algorithm estimates about 3.81 million people in total which is significantly higher than the lowest SpaceLiner numbers for this mission (0.07 million). Starship is only optimized for heat flux in the current optimization framework. It is feasible to fly a higher trajectory. However, this will result in a higher peak heat flux due to the steeper re-entry. As with the SpaceLiner, the actual overpressure level is not evaluated at this stage of the investigation, but is expected to be low in this case since the altitude of the vehicle is still fairly high.

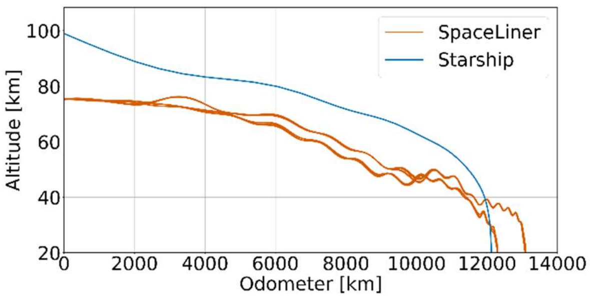

Fig. 12. Altitude-Odometer diagram between SpaceLiner and Starship for Brazil – India

Comparing the re-entry profile of both vehicles (see Fig. 13), Starship requires significantly more initial velocity to traverse the distance to the target location as it mostly relies on covering the distance in a ballistic arc. In contrast, SpaceLiner requires less energy while travelling further by utilizing the high lift-to-drag ratio at hypersonic velocities. During the final re-entry phase below 4 km/s, Starship and SpaceLiner follow a very similar profile.

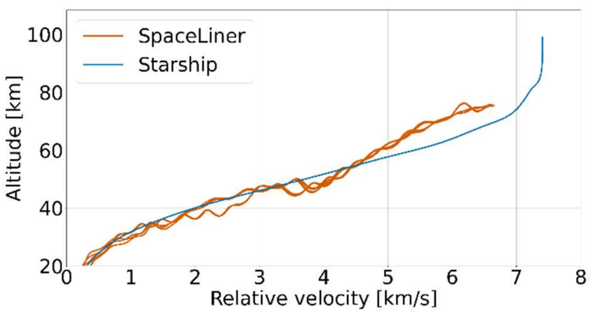

Fig. 13. Altitude-Velocity diagram between SpaceLiner and Starship for Brazil – India

In the reverse direction, India to Brazil, SpaceLiner flies on a similar route around Madagascar and South Africa as well as a similar re-entry profile (see world map in Fig. 9). In contrast, for Starship the optimizer is not able to find a feasible solution in a westward direction. It was not able to decrease the lateral loads below its constrained value.

Instead, when releasing the launch azimuth constraint at the launch site, a feasible solution is found flying eastwards. While the flown distance is more than doubled (about 26.000 km in comparison to 13.000 km), Starship largely benefits from launching and re-entering in the direction of Earth's rotation. The large impact of the launch azimuth for the Starship configuration is more generally investigated in [1].

During the re-entry, this may become a disadvantage as it is not able to use a curved route to avoid population. The re-entry will always be in the direction of the great circle connecting the launch and landing site. In this case, launching eastward results in overflying South America from west to east, which would cause large disturbances of the overflown areas. This might make the route unfeasible due to regulatory and safety concerns.

5. Conclusion

Both SpaceLiner and Starship offer unique potential for high-speed point-to-point transportation on Earth. In this study, their feasible trajectories are analysed and compared with an innovative multi-objective optimization method using evolutionary algorithms.

The use of a multi-objective optimization tool offers the possibility to significantly improve the trajectories based on the multitudes of constraints and objectives that can be set. Furthermore, utilizing databases like the population density map, the trajectories can be subjected not only to purely flight-related constraints and objectives, but also related to the surrounding environment.

For SpaceLiner, a multitude of trajectories are found that utilize the hypersonic lifting capability to avoid large populated areas around the world by strategically flying around them. These trajectories largely use the Oceans and/or the polar regions to arrive at the target location.

In contrast, the ability of the Starship to deviate from the great circle are limited. Additionally, it flies substantially higher into space than SpaceLiner. This allows Starship to avoid population disturbance in the middle of the flight and thus cross large populated landmasses. However, during re-entry, it cannot divert at all leading to a more limited flight route selection when applying the boundary conditions set for this study. Additionally, the trajectory design must compromise between a lower flight with a shallow re-entry and low heat flux or a higher flight leading to higher heat flux but managing to disturb less population.

In future work, besides finding more feasible routes, the location of some of the self-chosen launch and landing locations (apart from the official launch sites like

Cape Canaveral) shall be analysed in greater detail as this has a large impact on the flight routes available.

The topic of the sonic boom during ascent and descent also merits further investigation. A more detailed analysis of the affected population and the overpressure levels experienced would allow a better assessment of the level of disturbance caused during overflight.

Another topic that has to be investigated is the environmental and specifically atmospheric impact of these systems, especially if they were to fly regularly. As both the SpaceLiner and Starship create water vapor as exhaust, they have an impact on the upper atmospheric layers, which contributes to global warming [32]. If these effects are quantified, the optimizer could be adapted to also minimize the amount of water deposited in the critical altitudes. For the methane-fuelled Starship, the impact of the other exhaust gas components, including CO_2, have to be considered. Similar to work done in [33] for semi-reusable launch vehicles, the environmental impact for various point-to-point vehicles could be assessed.

Furthermore, the next step in the SpaceLiner design could be an adaptation towards a similar flight profile to Starship by adapting the wing design towards a long exoatmospheric coast with a single re-entry.

All in all, this study represents an important step in identifying and optimizing feasible point-to-point missions for rocket-propelled launch systems. The methodology can be used to assess other vehicles and missions as needed. For both reference vehicles missions were assessed and an understanding of the differences and similarities gained.

Acknowledgements

The authors gratefully acknowledge the contributions of Mr. Thomas Gandois and Mr. Michael Berger to the work performed in this study.

Part of this work was performed within the project ‘European Concept of Higher Airspace Operations’ (ECHO). This project has received funding from the SESAR Joint Undertaking (JU) under grant agreement No 890417. The JU receives support from the European Union’s Horizon 2020 research and innovation programme and the SESAR JU members other than the Union. Further information on ECHO can be found at https://higherairspace.eu/

References

[1] J. Wilken, S. Callsen: Mission design for point-to-point passenger transport with reusable launch vehicles, CEAS Space Journal (submitted), 2022

[2] M. Sippel, S. Stappert, Y. M. Bayrak, L. Bussler, S. Callsen: Systematic Assessment of SpaceLiner Passenger Cabin Emergency Separation Using Multi-Body Simulations, 2nd International Conference on High-Speed Vehicle Science Technology (HiSST), Bruges, Belgium 2022

[3] M. Sippel: Promising roadmap alternatives for the SpaceLiner, Acta Astronautica, Vol. 66, Issues 11-12, 2010

[4] M. Sippel, O. Trivailo, L. Bussler, S. Lipp, S. Kaltenhäuser, R. Molina: Evolution of the SpaceLiner towards a Reusable TSTO-Launcher, 67th International Astronautical Congress (IAC), Guadalajara, Mexico, 2016

[5] M. Sippel, J. Wilken: Preliminary Component Definition of Reusable Staged-Combustion Rocket Engine, Space Propulsion Conference, Seville, Spain, 2018

[6] M. Sippel, S. Stappert, V. Pastrikakis, V. Barannik, D. Maksiuta, L. Moroz: Systematic Studies on Reusable Staged-Combustion Rocket Engine SLME for European Applications, Space Propulsion Conference, Estoril, Portugal, 2022

[7] D. Neeb, T. Schwanekamp, A. Gülhan: Preliminary Aerodynamic Shape Optimization of the SpaceLiner by Means of Engineering Methods, 17th AIAA International Space Planes and Hypersonic Systems and Technologies Conference, San Francisco, USA, 2011

[8] M. Sippel, A. van Foreest, I. Dietlein, T. Schwanekamp, A. Kopp: Analyses Driving Improved Aerothermodynamic Lay-out of the SpaceLiner Configuration, ESA-SP692, 2011

[9] M. Sippel, T. Schwanekamp: The SpaceLiner Hypersonic System – Aerothermodynamic Requirements and Design Process, 8th European Symposium on Aerothermodynamics for Space Vehicles, Lisbon, Portugal, 2015

[10] G. Zuppardi, L. Morsa, R. Savino, M. Sippel, T. Schwanekamp: Rarefied aerodynamic characteristics of aero-space-planes: a comparative study of two gas-surface interaction models, European Journal of Mechanics B/Fluids, Volume 53, pp. 37-47, https://doi.org/10.1016/j.euromechflu.2015.04.003, 2015

[11] M. Sippel, S. Stappert, S. Singh: RLV-Return Mode “In-Air-Capturing” and Definition of its Development Roadmap, 9th European Conference for Aeronautics and Space Sciences (EUCASS), Lille, France, 2022

[12] SpaceX: Starship, https://www.spacex.com/vehicles/starship (accessed August 2022)

[13] SpaceX (YouTube): Starship Update, 11th February 2022, https://www.youtube.com/watch?v=3N7L8Xhkzqo (accessed August 2022)

[14] SpaceX (YouTube): Starship | Earth to Earth, 29th September 2017,

https://www.youtube.com/watch?v=zqE-ultsWt0 (accessed August 2022,)

[15] Official SpaceX Photos (Flickr): Starship Super Heavy, 10th February 2022, https://www.flickr.com/photos/spacex/51924610024 (accessed August 2022)

[16] J. Wilken, M. Berger, M. Sippel: Critical Analysis of SpaceX's Next Generation Space Transportation System: Starship and Super Heavy, 2nd International Conference on High-Speed Vehicle Science Technology (HiSST), Bruges, Belgium, 2022

[17] J. Roshanian, A. A. Bataleblu, M. Ebrahimi: Robust ascent trajectory design and optimization of a typical launch vehicle, Journal of Mechanical Engineering Science, Volume 232, Issue 24, Pages 4601-4614, 2018

[18] R. Chai, A. Savvaris, A. Tsourdos, S. Chai: Multi-objective trajectory optimization of Space Manoeuvre Vehicle using adaptive differential evolution and modified game theory, Acta Astronautica, Volume 136, Pages 273-280, 2017

[19] M. A. Vavrina, J. A. Englander, S. M. Phillips et al.: Global, Multi-Objective Trajectory Optimization with Parametric Spreading, AAS/AIAA Astrodynamics Specialist Conference, 2017

[20] L. Brevault, M. Balesdent, A. Hebbal: Multi-Objective Multidisciplinary Design Optimization Approach for Partially Reusable Launch Vehicle Design, Journal of Spacecraft and Rockets, Volume 57, No. 2, 2020

[21] R. L. Speth, S. D. Eastham, T. M. Fritz et al.: Global Environmental Impact of Supersonic Cruise Aircraft in the Stratosphere, NASA/CR-20205009400, 2021

[22] R. Strom, K. Price: Differential Evolution – A Simple and Efficient Heuristic for global Optimization over Continuous Spaces, Journal of Global Optimization 11, pp. 341-359, 1997

[23] K. Deb: Multi-Objective Optimization Using Evolutionary Algorithms, Wiley, New York, USA, 2011

[24] F. Bre, V. D. Fachinotti: A computational multi-objective optimization method to improve energy efficiency and thermal comfort in dwellings, Energy and Buildings, Volume 154, pp. 283 – 294, https://doi.org/10.1016/j.enbuild.2017.08.002, 2017

[25] Center for International Earth Science Information Network – CIESIN – Columbia University, 2016, Gridded Population of the World, Version 4 (GPWv4): Population Density, Palisades, NY: NASA Socioeconomic Data and Applications Center (SEDAC), http://dx.doi.org/10.7927/H4NP22DQ (accessed August 2022)

[26] H. W. Carlson: Simplified Sonic-Boom Prediction, NASA Technical Paper 1122, Langley Research Center, Hampton, Virginia, USA, 1978

[27] D. J. Maglieri, P. J. Bobbitt, K. J. Plotkin et al.: Sonic Boom – Six Decades of Reseach, NASA/SP-2014-622, Hampton, Virginia, USA, 2014

[28] Firefly Aerospace: Alpha Payload User Guide, rev. 3.1, April 2022, https://firefly.com/wp-content/uploads/2022/05/Alpha-PUG-3.1.pdf (accessed August 2022)

[29] Air Force Space Command Manual 91-710, Volume 1, November 2016, https://static.e-publishing.af.mil/production/1/spoc/publication/afspcman91-710v1/afspcman91-710v1.pdf (accessed August 2022)

[30] ESA: The CSG 2000 Programme, https://www.esa.int/esapub/bulletin/bullet83/csg2083.htm (accessed August 2022)

[31] M. Kummu, O. Varis: The world by latitudes: A global analysis of human population, development level and environment across the north-south axis over the past half century, Applied Geography, Volume 31, pp. 495 – 507, https://doi.org/10.1016/j.apgeog.2010.10.009, 2011

[32] S. Solomon, K. H. Rosenlof, R. W. Portmann et al.: Contributions of Stratospheric Water Vapor to Decadal Changes in the Rate of Global Warming, Science, Volume 327, 2010

[33] L. Miraux, A. R. Wilson, G. J. Dominguez Calabuig: Environmental sustainability of future proposed space activities, Acta Astronautica, Volume 200, Pages 329-346, 2022